

Spin polarized electron transport and emission from strained
semiconductor heterostructures^{*}

Yu. A. Mamaev, A. V. Subashiev, Yu. P. Yashin and A. N. Ambrajei
State Technical University, 195251, St.-Petersburg, Russia

H.-J. Drouhin and G. Lampel
Laboratoire PMC, UMR 7643-CNRS, Ecole Polytechnique, 91128, Palaiseau, France

J. E. Clendenin, T. Maruyama and G. A. Mulhollan
Stanford Linear Accelerator Center, Stanford University, Stanford CA 94309

*Presented at the International Workshop on
Physics of Low Dimensions,
Oaxaca, Oax., Mexico,
January 16-20, 2000*

^{*} Work supported by Department of Energy contract DE-AC03-76SF00515.

Yu. A. Mamaev, A. V. Subashiev, Yu. P. Yashin and A. N. Ambrajei
State Technical University, 195251, St.-Petersburg, Russia
H.-J. Drouhin and G. Lampel
Laboratoire PMC, UMR 7643-CNRS, Ecole Polytechnique, 91128, Palaiseau, France
J. E. Clendenin, T. Maruyama and G. A. Mulhollan
Stanford Linear Accelerator Center, Stanford, CA 94309, USA

E-mail: mamaev@spes.stu.neva.ru

Abstract

High resolution energy distribution curves (EDC) and a polarization versus energy distribution curves (PEDC) of the electrons, photoemitted from strained GaAs/GaAsP layers are experimentally studied. In the vicinity of the photoexcitation threshold the polarization does not vary across the energy distribution, which means that no depolarization occurs during energy relaxation in the band bending region (BBR). The electron energy distribution is interpreted in terms of the electron energy relaxation in the band tail states of quantum well formed by the BBR. Polarized electron emission from a series of new strained short-period AlInGaAs/AlGaAs superlattices (SL) is investigated as well. The In layer content was chosen to give minimal conduction-band offset with large strain splitting of the V-band. Simultaneous changing of Al content in both SL layers provides variation of the structure band gap. We demonstrate as well that tuning of the SL to the excitation energy can be achieved without loss of the electron polarization. The polarization of up to 84% was measured at room temperature.

The sources of highly polarized electron beams are actively investigated in a view of their successful and growing applications in high energy physics, atomic physics, studies of thin film, and surface magnetism [1]. In order to produce highly polarized electrons strained GaAs layers on GaAsP pseudo-substrates are most frequently used. The strain-induced valence-band splitting leads to very high (close to 100%) initial electronic optical orientation under excitation by circularly polarized light at the inter-band absorption edge. The emission of polarized electrons in vacuum is provided by activation of the clean GaAs surface by Cs(O) deposition which drastically reduces the electron work function and leads a negative electron affinity (NEA) surface formation.

Near-threshold emission from strained GaAs/GaAsP layer

The polarized electron photoemission from the stressed film is understood as a multi-step process, consisting of: (i) electron excitation under optical pumping, (ii) electron energy relaxation to the local equilibrium state, (iii) capture in the band bending region (BBR), then (iv) energy relaxation in the potential well formed by the band-bending region and, finally (v) electron escape into vacuum throughout the weakly transparent surface barrier formed by the activation layer.

The minimum energy of the EDC's are determined by the vacuum level achieved during the activation procedure and the aging processes, whereas the maximum energy corresponds to the ballistic emission of electrons photoexcited from the uppermost valence band level to the conduction band. The precise shapes of the EDC's are determined by the electron kinetic, the details of which are still not completely understood, specially steps (iii - v). For bulk unstrained GaAs, activated to NEA, the EDC's peak at an energy a few hundreds of millivolt below the bottom of the conduction band is observed revealing the effectiveness of energy relaxation in the BBR [2-5]. For excitation energies *close* to the band gap the polarization of the emitted electrons is essentially constant throughout this distribution and its value decreases with increasing $h\nu$. For *higher* excitation energies the polarization tends to increase at large kinetic energies where electrons are emitted without any energy or spin relaxation [2].

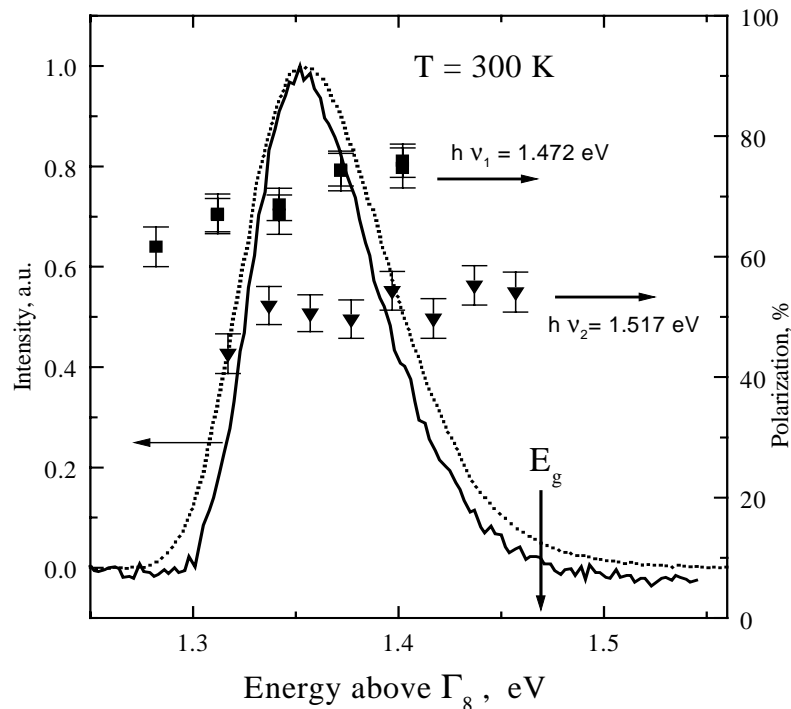
Additional information is obtained in thin-layer cathodes [6] when the electron emission times are comparable to the energy relaxation times either in the active layer or on the BBR so that a large fraction of electrons are emitted prior to complete thermalisation. The PEDC's reflect the spin relaxation kinetics.

In the paper [7] the first experimental results for energy and polarization distribution curves of electrons photoemitted from a highly strained GaAs layer were reported. We show that the results for near band-gap excitation are in line with the model of highly localised electron states in the BBR.

Experimental results. The experimental set-up was described in [2]. The sample is illuminated by σ^+ or σ^- circularly polarized light from a Ti:Sapphire or He-Ne laser normal to its surface. The photoemitted electrons are energy selected by a cylindrical 90° electrostatic deflector operating in the constant-energy mode. The full width at half maximum of the transmission function is $\Delta E = 20$ meV. The polarization of the energy-selected electrons is measured by Mott scattering on a gold foil at the voltage 30 or 100 kV. NEA state was achieved by activation of atomically clean surfaces with cesium and oxygen. The thermal cleaning procedure (at residual pressure not exceeding $1 \cdot 10^{-9}$ Torr) consisted of gradual heating of the samples up to 400° C and 30 min exposition at this temperature, then heating up to 500° C and 30 min exposition and finally the heating up to 620° C with 1 hour exposition at this temperature. The value of a sample temperature was controlled by a thermocouple. The structure of the sample under investigation was described in [8]. A 140 nm thick GaAs overlayer is MOCVD grown on a $\text{GaAs}_{0,72}\text{P}_{0,28}$ buffer at the top of commercial GaAs (001) wafer. To reduce the overlayer relaxation effects, a special type of heterostructure with the intermediate $\text{GaAs}_{0,55}\text{P}_{0,45}/\text{GaAs}_{0,85}\text{P}_{0,15}$ superlattice has been used. As a result a strain-induced energy splitting of $\delta \approx 40$ meV in the valence band has been achieved so that high values of the photoelectrons spin polarization of $\geq 80\%$ at room temperature were reached even after several re-activation cycles.

The EDC and PEDC data at room temperature for *near band-edge excitation* are presented in Fig. 1. The position of the EDC peak is shifted below the conduction band edge as in the most of unstressed GaAs cathodes, though, EDC are rather narrow (FWHM does not exceed 100 meV) at room temperature and do not change much at 120 K. The shape of the EDC peak remains almost unchanged in the excitation range in the vicinity of the phototreshold $E_g - 0.02 \text{ eV} \leq h\nu \leq E_g + 0.07 \text{ eV}$, where $E_g = 1.47 \text{ eV}$. The observed shapes of the EDC are typical for the cathodes with two-stage surface activation procedure [4,5]. It is clearly seen that the polarization remains constant across EDC, so that no depolarization effects for the electrons in BBR region are registered. As a result the integrated values of the electron polarization for the $P(h\nu)$ spectrum and the P values measured at the EDC maximum (both at 20, and 80 meV resolutions) are found to be about equal at given $h\nu$.

Fig.1. Polarized electron distributions and electron energy distributions of the emitted



electrons for GaAs/GaAsP strained cathode. EDCs (solid line - $h\nu = 1.472 \text{ eV}$; dots - $h\nu = 1.517 \text{ eV}$) are normalised to the maximum value. $T = 300 \text{ K}$, energy resolution is 20meV. Band gap value of the strained overlayer is shown by arrow.

Discussion. In the case of near band-edge excitation, $h\nu - E_g \leq kT$, as it is evidenced by Fig. 1, the electrons are captured in BBR prior to the emission. Monte-Carlo modelling of the spatial distribution of the electron potential in BBR [9] reveals large fluctuations of the electronic potential at the surface, originated from randomly distributed ionised acceptors and Cs- originated donor centres. This implies that all the electronic states in the BBR below a certain energy defined as an electron Mobility Edge (ME) are localised also in the surface plane by the potential fluctuations. The density of the localised states $g(\varepsilon)$ below the ME is a rapidly decreasing function of the localisation energy ε in the bang gap (measured downwards from the ME). The estimated and measured time of the electron emission from the BBR in vacuum $\tau_{emi} \approx 5 \text{ ps}$ is much larger than the time of the delocalised electron

energy relaxation due to the emission of the phonons $\tau_{po}=1.5 \cdot 10^{-13}$ s. Therefore the experimental results can be analysed in terms of a model that consider the EDC formation as a result of competition of the processes of the electron emission in vacuum and the electron hopping in tail states with emission of the optical phonons. The model was developed in [10] for interpretation of the luminescence spectra in mixed crystals and generalised in [11] for electron emission from BBR.

In this model $g(\varepsilon)$ is approximated by an exponential law with an energy width γ . Therefore, below the ME, the probability for an electron to emit a phonon is proportional to $\exp(-\varepsilon/\gamma)$ and the electron energy relaxation is rapidly suppressed

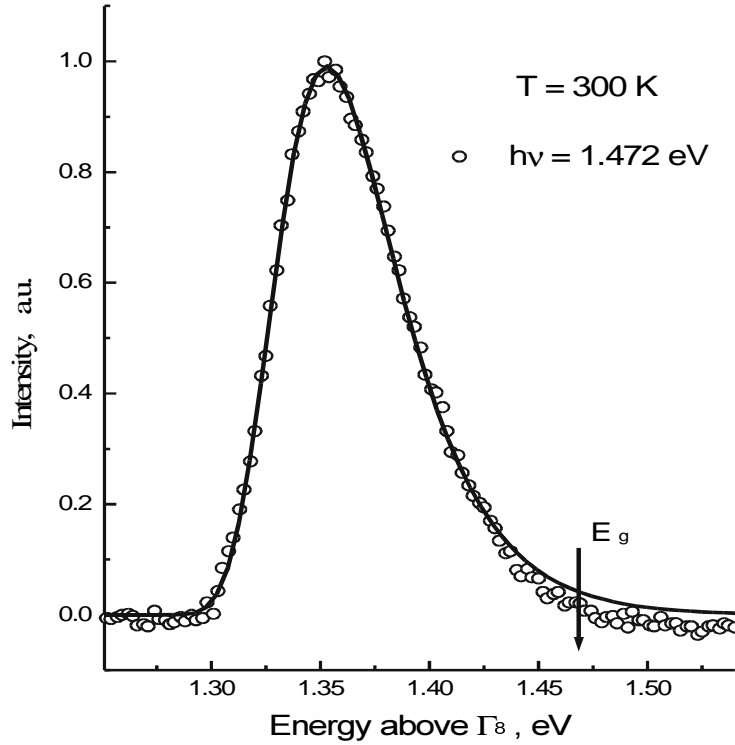


Fig. 2. Experimental electron energy distribution curve at $T = 300$ K, together with the results of the calculations (solid line) using Eq. (2) of the localised states model with $\gamma=28.7$ meV and $\alpha=0.11$. Band gap value is shown by arrow.

because of the lack of resonant localised final states in the vicinity of the occupied one. To be more specific, we assume that the main energy relaxation process is by phonon emission with an average energy loss δ much smaller than γ and with a probability $\tau^1(\varepsilon) = \tau^1(0)\exp(-\varepsilon/\gamma)$. It is then possible to write the energy relaxation for the electronic surface density $n(\varepsilon)$ as a Fokker-Planck type equation:

$$\partial n/\partial t = -\delta \cdot \partial/\partial \varepsilon \{ n(\varepsilon)/\tau(\varepsilon) \} - n(\varepsilon)/\tau_{emi} \quad (1)$$

In this equation the first term describes the flow of electrons through the states with energy ε : $n(\varepsilon - \delta)/\tau(\varepsilon - \delta) - n(\varepsilon)/\tau(\varepsilon)$ and the second one is just the emission current $J_{emi}(\varepsilon)$. In stationary conditions $\partial n/\partial t = 0$ and one obtains the energy dependence of the emission current in the BBR

$$J_{emi}(\varepsilon) = J_{emi}(0) \exp \{ \varepsilon/\gamma - \alpha \cdot [\exp(\varepsilon/\gamma) - 1] \} \quad (2)$$

where the parameter α is given by $\alpha = (\gamma/\delta) \cdot [\tau(0)/\tau_{emi}]$.

The results of the calculations of the EDC together with the experimental curve are shown in Fig. 2. We use fitting of the Eq. (2) dependence to experimental data to estimate the energy relaxation rate in BBR by the phonon emission. First, we note that the value of $\gamma=28.7$ meV obtained from the fitting is found to be not dependent on the choice of α , whereas the value of α depends on the assumed position of the ME level in BBR below the conduction band. In 2-d system the low-energy shift of ME should be close to γ value. So, we take the position of zero in Eq. (2) at $E_c - \gamma$ (conduction band edge E_c being at 1.47 eV in the doped strained layer) which results in $\alpha=0.11$.

Then, for the localised states the phonon emission rate at ME $1/\tau(0)$ is equal to the probability of a single jump multiplied by the number of final states, that is, $1/\tau(0) = 1/\tau_{ph} \delta g_0 \pi a^2$, where g_0 is the surface electron density of states at ME, a is an average radius of localised states, so that $g_0 \pi a^2 \gamma \approx 1$. That gives $1/\tau(0) = 1/\tau_{ph} \delta \gamma$ and $\alpha = (\gamma/\delta)^2 \cdot (\tau_{ph}/\tau_{emi})$. Taking $\delta \gamma = 0.3$ we get $\tau_{ph} \approx 50$ fs, which is in reasonable agreement with the data for the energy relaxation rate for hot electrons in a narrow p-doped GaAs quantum well [12].

Finally, note, that the main spin-relaxation mechanism of D'yakonov-Perel (DP) is suppressed for the localised states due to the effective averaging of the odd in k -vector terms in DP Hamiltonian at all directions, so that $\langle k_i k_j k_l \rangle = 0$. Besides, the weak overlap of the electron localised states with hole states out of BBR makes Bir-Aronow-Pikus relaxation due to electron scattering on the holes ineffective. Thus observed depolarization switching off below the conduction band energy is in line with the assumption of localisation of electronic states in this energy region.

Strained Al In Ga As/Al Ga As superlattices with a minimal conduction-band offset

It has been found that there is a limit to current density that can be extracted from a GaAs film [13], which results from the photovoltage effects in the band-bending region near the activated surface. A new generation of highly polarized electron sources is associated with semiconductor superlattice structures in which the valence band splitting is achieved as a consequence of hole confinement in the SL quantum wells (QW). The main advantage of SL-based photoemitters is the possibility to vary the properties of the active layer over a wide range by the appropriate choice of layer composition, thickness, and doping profile [1,14].

Recently a new strained short-period $\text{Al}_x\text{In}_y\text{Ga}_{1-x-y}\text{As}/\text{Al}_z\text{Ga}_{1-z}\text{As}$ superlattice with a minimal conduction-band offset was proposed [1]. The main advantage of the SL results from the band line-up between the semiconductor layers of the SL. The Al content determines the formation of a barrier in the conduction band, while adding In leads to conduction band lowering, so the conduction band offset can be completely compensated by appropriate choice of x and y , while barriers for the holes remain uncompensated. As a result a high vertical electron mobility and simultaneously a small spin relaxation rate is achieved while also a large enough valence-band splitting is remained. Additional improvement of the emitter parameters is expected for the SLs with wider band gap. Wider gap ensures higher NEA and therefore higher quantum yield and emitted currents. We show that the performance of this new superlattice exceeds that of the GaAs strained layer cathodes while tuning of the band gap gives additional advantages.

The SL samples were grown by solid-source molecular beam epitaxy on GaAs(100)-oriented substrates. The SL samples consisted of 12-15 pairs of AlGaAs (4 nm) and AlInGaAs (4 nm) doped with Be and were terminated by a 6 nm (or 8 nm) heavily-doped GaAs layer capped with As to ensure stable activation and an NEA surface state. The parameters of the samples are listed in Table 1. All the samples were capped by As for the surface protection. The As cap thickness was estimated to be 0.1 nm based on Auger profiling measurements. The characterisation of the samples was done using luminescence and X-ray diffraction techniques. The X-ray diffraction patterns show that in the case of the GaAs substrate and $x \leq 0.2$, the strain relaxation in the thin 4-nm $\text{Al}_x\text{In}_y\text{Ga}_{1-x-y}\text{As}$ layers remains negligible for the total SL thickness, d , up to $d \leq 150$ nm.

Table 1. $\text{Al}_x\text{In}_y\text{Ga}_{1-x-y}\text{As}/\text{Al}_z\text{Ga}_{1-z}\text{As}$ strained superlattice samples.

Sample	SL1 (3-336)	SL2 (3-657)	SL3 (3-895)	SL4 (3-896)
Be doping:				
Surface	$7 \cdot 10^{18}$	$2 \cdot 10^{19}$	$5 \cdot 10^{19}$	$5 \cdot 10^{19}$
Inside	$4 \cdot 10^{17}$	$5 \cdot 10^{17}$	$5 \cdot 10^{17}$	$5 \cdot 10^{17}$
$d, \mu\text{m}$	0.136	0.12	0.96	0.96
$x, \%$	20	30	30	32
$y, \%$	18	18	18	18
$z, \%$	0	10	14	17
$E_{\text{ex}}(\text{pol.max}), \text{eV}$	1.45	1.54	1.58	1.6
max P, %	82.7	83	84	81
$Y(\text{pol.max}), \%$	0.094		0,1	0,09

Choice of the SL layer composition. The miniband spectrum of the SL is determined by the band offsets at the heterointerfaces. In the case of a heterointerface with lattice matched ternary solid solution (e.g. $\text{Al}_x\text{Ga}_{1-x}\text{As}-\text{Al}_z\text{Ga}_{1-z}\text{As}$) the conduction-band offset ratio, Q_{c1} , defined as $Q_{c1} = \Delta E_c(x-z) / \Delta E_{g1}(x-z)$ (where $\Delta E_{g1}(x)$ is the difference in the band gaps of the contacting crystals) is known to remain constant, $Q_{c1} \cong 0.66$. For an $\text{In}_y\text{Ga}_{1-y}\text{As}-\text{GaAs}$ interface the offset is modified by the strain distribution in the contacting layers. For the structure with a thin $\text{In}_y\text{Ga}_{1-y}\text{As}$

layer grown on a thick GaAs substrate all the strain is assumed to accumulate in the InGaAs layer. For the case of the $\text{Al}_x\text{In}_y\text{Ga}_{1-x-y}\text{As}/\text{Al}_z\text{Ga}_{1-z}\text{As}$ SL, a linear interpolation between the values for $\text{Al}_x\text{Ga}_{1-x}\text{As}-\text{GaAs}$ and $\text{In}_y\text{Ga}_{1-y}\text{As}-\text{GaAs}$ interfaces should be valid for small x and y . The schematic of the position of the band edges for $x=0.30$, $y=0.18$, $z=0.1$ is shown in Fig. 3.

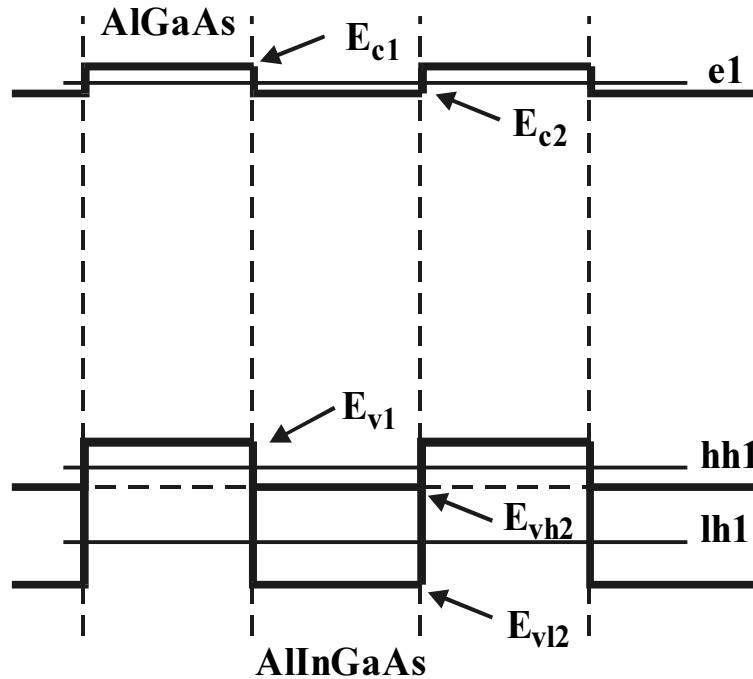


Fig.3. Energy band diagram of $\text{Al}_x\text{In}_y\text{Ga}_{1-x-y}\text{As}/\text{AlGaAs}$ superlattice. The minibands (thin lines) are identified by notation $e1$ and $hh1$, $lh1$ for electrons and holes respectively.

We have found that for taken band offset parameters the conduction band offset appears to be minimised for $z = 1.1 (x-1.1y)$. For the thermalised electrons at room temperature the influence of the resulting periodical potential should be negligible. Besides, as a result of the conduction-band line up, the 4-nm barriers for the electrons in the SL are transparent. Thus the changes of electron mobility and spin relaxation rate should be small compared to pure GaAs. Using the structures based on quaternary $\text{Al}_x\text{In}_y\text{Ga}_{1-x-y}\text{As}$ alloy one can change the band gap by varying the Al content in the layers while In concentration remains unchanged to keep high deformation and strain-induced valence band splitting. It is seen from Fig.3 that the strain of the $\text{Al}_x\text{In}_y\text{Ga}_{1-x-y}\text{As}$ layers produces barriers for both heavy and light holes, the barrier for the light holes being 75meV higher, which leads to additional hole-miniband splitting favourable for the electron optical orientation. The choice of the layer thickness is dictated by the need to split the hole minibands. The splitting grows when barriers are broad enough and wells are narrow and deep.

Experimental results and discussion. The Mott analysers both at St.-Petersburg Technical University (SPTU) and at the Stanford Linear Accelerator Centre (SLAC) were used to measure the spin polarization of photoelectrons. In Fig. 4 the polarized emission data are shown as a function of the optical excitation energy. The maximum polarization obtained with local optical excitation was 84% and the corresponding quantum yield, Y , was 0.1 %. The observed emission spectra can be interpreted in terms of a three-step model linearised for the thin-film emitter case [15]. The

polarization dependence on the excitation energy near the excitation edge comes from the initial electron polarization upon excitation by circularly polarized light. The decrease of the polarization from its maximum value with decreasing excitation wavelength starts with electron excitation from the first light-hole miniband.

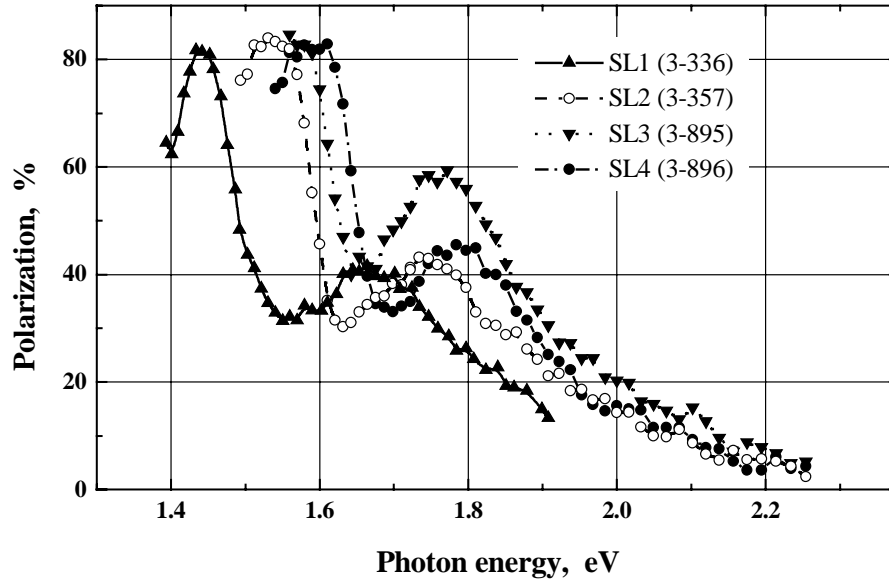


Fig. 4. Electron spin polarization spectra for $\text{Al}_x\text{In}_y\text{Ga}_{1-x-y}\text{As}/\text{Al}_z\text{Ga}_{1-z}\text{As}$ superlattices.

The fall off of polarization as excitation drops below the conduction band minimum can be associated with electron excitation in indirect transitions with electron scattering on the defects or with absorption of the optical phonon in which electrons with both orientations of electron spin are created in the conduction band. A sharp decrease of Y and P below the band edge indicates good quality of the structures.

Thus, the position of the polarization maximum is close to the SL band gap. In the SL the band gap is larger than that in GaAs layers by quantisation energy of the heavy holes and some shift of the conduction band minimum. Calculation of the miniband energies for SL-1 using the model described in [16] gives absolute values of the hole miniband energies $E_{\text{hh1}}=13$ meV ; $E_{\text{lh1}}=54$ meV. Therefore the splitting of the valence band is close to 40 meV and it does not change much with simultaneous changes of Al content in both SL layers. The edge of the electronic band in a SL with a small conduction-band offset is close to the average conduction -band energy in the contacting layers.

The calculation of the band gap using the data given in Table 1 gives for all samples values that exceed the experimentally observed energy of the polarization maximum by ~ 20 meV. This shift of the band gap values is equivalent to a deficit of $\approx 3\%$ of Al concentration. The regular difference in the calculated and observed band gap value in the strained quaternary alloy can be attributed to the uncertainties in the conduction band offset calculations and also to some tensile deformation of GaAs layer resulting in less strain in the contacting $\text{Al}_x\text{In}_y\text{Ga}_{1-x-y}\text{As}$ layer. This misfit can be rather easily corrected by choosing a SL with larger x when some tuning of the SL band gap to excitation source is needed. Indeed, adding of Al does not influence the deformation so that the band gap variation with x is predictable.

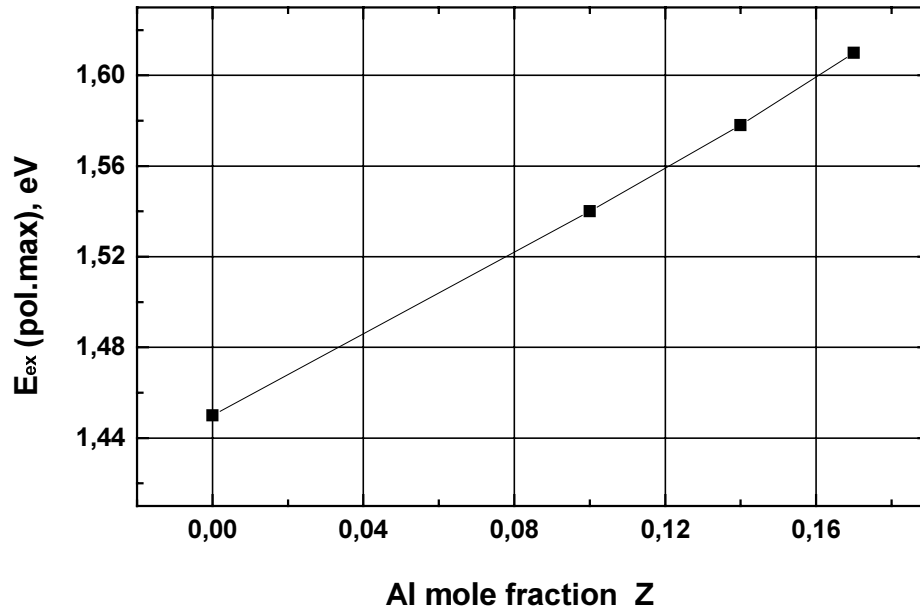


Fig. 5. The values of the light energy E_{ex} (pol. max.), corresponding to the polarization maximum as a function of the mole fraction Z of Al in the $Al_xIn_yGa_{1-x-y}As/Al_zGa_{1-z}As$ superlattice.

The dependence of the polarization maximum on the excitation energy is shown in Fig 5. Linear dependence is found that makes possible the tuning of the maximum to the excitation wavelength. One can expect larger splitting with thicker barriers and thinner AlGaAs wells. Then, one can expect a smaller spin relaxation rate for optimally chosen doping of the SL, compatible with needed extracted emission current. Thus, the optimisation of the SL structure parameters and doping profile can lead to further improvement of the proposed new SL photoemitter structure. Finally, the maximum current density that can be extracted from these SL samples at high voltage has yet to be determined. Initial measurements using sample 1 gave anomalously low value. Definitive measurements are underway.

Conclusions

The EDC and PEDC measurements for the strained GaAs layer surface activated to NEA, at near band edge excitation demonstrate the electron capture to the band bending region before emission. The shape of the energy distribution peak is in good agreement with the results of the model of the emission from the states localised in the surface plane by the fluctuations of the surface potential. The localisation is also manifested by switching off the spin relaxation across the emission peak.

Electron spin polarization as high as 84% has been reproducibly obtained from strained $Al_xIn_yGa_{1-x-y}As/Al_zGa_{1-z}As$ superlattices with small conduction band offset at

the heterointerfaces. The position of the polarization maximum varies linearly with Al concentration and can be easily tuned to an excitation wavelength by choice of the SL composition. Conduction band offset at $\text{Al}_z\text{Ga}_{1-z}\text{As}/\text{Al}_x\text{In}_y\text{Ga}_{1-x-y}\text{As}$ interface changes its sign at $z \cong 1.1(x-1.1y)$. The modulation doping of the SL is found to be essential for high polarization and high quantum yield at the polarization maximum. Further improvement of the emitter parameters can be expected with additional optimisation of the SL structure parameters.

References

1. See e.g., A.V.Subashiev, Yu.A.Mamaev, Yu.P.Yashin, and J.E.Clendenin, *Phys. Low-Dim. Structures* **1/2**, 1 (1999), and references therein.
2. H.-J.Drouhin, C.Hermann, G.Lampel, *Phys. Rev.* **B31**, 3859 (1985) ; **B31**, 3872 (1985).
3. A.S. Terekhov and D.A. Orlov, *Proc. SPIE* **2550**, 157 (1995).
4. A.W.Baum et al., *Proc. SPIE* **2550**, 189 (1995).
5. E.L.Nolle, *Sov.Phys.-Solid State*, **31**, 196 (1989).
6. F. Ciccacci, H.-J. Drouhin, C. Hermann, R. Houdre and G. Lampel, *Appl. Phys. Lett.*, **54**, 632 (1989).
7. Yu.A.Mamaev, A.V.Subashiev, Yu.P.Yashin, H.-J.Drouhin and G.Lampel, *Solid State Comm.*, (2000), accepted for publication.
8. Yu.A.Mamaev, Yu.P.Yashin, A.V.Subashiev et al., *Phys. Low-Dim. Structures* **7**, 27 (1994).
9. B.D. Oskotskij, A.V. Subashiev and L.G., in *AIP Conference Proceedings CP421*, Polarized Gas Targets and Polarized Beams, 7-th Intern. Workshop, Urbana, ed. R. Holt et al. 1998, p. 491.
10. E.L. Ivchenko, M.I. Karaman, D.K. Nelson et al., *Phys. Solid State* **36**, 218 (1994).
11. A.V.Subashiev, *Proc. of the Low Energy Polarized Electron Workshop LE-98*, St.-Petersburg, 1998, edited by Yu.A.Mamaev et al., SPES-Lab-Pub., 1998, p. 125.
12. D.N. Mirlin, V.I. Perel', I.I. Reshina, *Semiconductors*, **32**, 886 (1998).
13. H.Tang et. al., *Proc. of the 4th European Particle Accelerator Conf.*, May 17-23, 1994, London, UK, World Scientific, Singapore, 1994, p.46.
14. K.Togawa et al., *Nucl. Instrum. and Meth.* **A414**, 461 (1998).
15. B. D. Oskotskij, A. V. Subashiev and Yu. A. Mamaev, *Phys. Low-Dim. Structures*, **1/2**, 77 (1997).
16. L.G.Gerchikov, G.V.Rozhnov, A.V.Subashiev, *Sov. Phys. JETP* **74**, 77 (1992).